Supporting Information

SI Materials and Methods

Plasmid Construction and Genetic Transformation

For overexpressing miRNA, the precursors of *miR172b*, *miR529a* and *miR529b* were isolated by PCR using their corresponding primers. The PCR products were cloned into the *Kpn*I-*Bam*HI sites of pCAMBIA1301S or pCAMBIA1301U resulting in the overexpression vector.

For producing the target mimicry lines of *miR156* and *miR172*, the cDNA of *AtIPS1* was isolated from the *Arabidopsis thaliana Col* ecotype using the primers IPS1F (with *Kpn*I site) and IPS1R (with *Bam*HI site). The PCR fragment was cloned into the pGEM-T Easy vector (TransGen Biotech, China) resulting in pGEM-IPS1. Next, the partially complementary sequence of *miR156* and *miR172* were fused into GEM-IPS1 by overlap extension PCR using primers MIM156F/MIM156R and MIM172F/MIM172R resulting in IPS1-MIM156 and IPS1-MIM172 respectively, and these recombinant sequences were cloned into the *Kpn*I-*Bam*HI sites of pCAMBIA1301S for overexpression under the control of 35S promoter.

To generate the RNAi constructs, the fragments of *SPL14*, *SPL17*, *SNB*, *OsIDS1*, *OsTOE1*, *LAX1*, *RFL* and *ASP1* were isolated by PCR using the corresponding primers of each gene, and all the fragments were cloned into the *Kpn*I-*Bam*HI and *Spe*I-*Sac*I sites of the RNAi construct ds1301 (1).

To overexpress *SPL7*, *SPL14*, *SPL17*, *OsTOE1*, *RCN1*, the open reading frames (ORFs) of these genes were amplified from cDNAs using gene-specific primers. After subcloning and sequencing, the correct gene fragments were inserted into pCAMBIA1301S. To make the constructs for *SPL14GFP*, the ORF of *SPL14* without stop codon was fused to *GFP* and inserted in pCAMBIA1301S. For the construct *SPL7:rSPL7-HA*, the *miR156* binding site in *SPL7* was changed by overlap extension PCR and fused with two copies of *HA* tags, a 2.4-kb promoter fragment of *SPL7* was amplified separately and inserted into pCAMBIA1300 together with the recombinant

ORF. For the construct *rSNBOE*, the *miR172* binding site in *SNB* was changed by overlap extension PCR, and the resistant ORF was fused to *GFP* and inserted in pCAMBIA1301S.

To obtain the expression vector for purifying the protein GST-SPL14N, the gene fragment coding for the N-terminal 186 amino acids of *SPL14* was isolated by PCR and cloned into the *Eco*RI-*Sal*I site of pGEX-4T-1.

For yeast one-hybrid (Y1H) assay, the ORF of *SPL14* was isolated by PCR and cloned into the *Eco*RI-*Xho*I site of the vector pB42AD (Clontech, USA). The promoter fragment of *pri-miR172b*, *-miR172d*, *PAP2* and *LAX1* were isolated by PCR and cloned into the *Eco*RI-*Xho*I site of the vector pLacZi2μ (2).

For yeast two-hybrid (Y2H) assay, the ORFs of *SNB*, *OsIDS1*, *OsTOE1*, *ASP1* and *TPR1* were isolated by PCR and cloned into the vector pGBKT7 (Clontech, USA) and pGADT7 (Clontech, USA) respectively. The overlap extension PCR was employed to change the EAR motifs of SNB, OsIDS1 and OsTOE1, and to delete the CTLH domain of ASP1, and the mutated or truncated genes were cloned into the vectors as the entire ORFs.

To make the vectors for luciferase (LUC) complementation imaging assay, the ORFs of *SNB*, *OsIDS1*, *OsTOE1* and *ASP1* were cloned into the vectors pUC19-nLUC and pUC19-cLUC respectively (3). For BiFC analysis, the ORFs of *ASP1* and *SNB* were cloned into the vector pCAMBIA1300-nYFP and pCAMBIA1300-nCFP respectively.

For detecting the interaction between *miR529* and SPL genes, the precursors of *miR529a*, *miR529b* and *AtmiR172a* were cloned into the vector PM999, the *miR529* recognition site of *SPL17* was cloned into the vector pGEM-LUC (2).

All the primer sequences were in the Dataset S2.

Agrobacterium tumefaciens (*EHA105*) was used for rice transformation (4). Co-segregation analysis between the transgene and phenotype was performed using plants in the T1 generation for evaluating the effects of all the transgenes.

RNA Extraction and qRT-PCR

RNA was isolated using RNA extraction kit TRIzol (Invitrogen, USA) and quantified with Nanodrop (Thermo, USA). Transcript abundance was analyzed as previously described (5). Briefly, approximately 3 μg of total RNA was used for synthesizing the first-strand cDNA. qRT-PCR was performed with the SYBR Premix ExTaq kit (Takara, Japan) in a total volume of 25 μl on the Applied Biosystems 7500 Real-time PCR System following the manufacturer's manual. Data were normalized to the internal rice *ubiquitin* (*UBQ*) gene. And the relative quantification method was used for data analysis (6). For quantification of mature *miR156*, *miR172*and *miR529*, stem-loop reverse transcription quantitative PCR (7) was performed. *U6* snRNA was used as the internal control for normalizing the raw data.

Recombinant Protein Purification

GST and GST-SPL14N recombinant proteins were induced by 1 mM Isopropyl β-D-1-Thiogalactopyranoside (IPTG) and expressed in the *Escherichia coli* Transetta (DE3) strain (TransGen Biotech, China). The proteins were purified using Glutathione Sepharose 4B beads (GE Healthcare, USA) according to the manufacturer's manual.

EMSA

For EMSA, two complementary oligonucleotides of each probe were synthesized and labeled with biotin separately, and double strand probes were obtained by annealing the two oligonucleotides. For each reaction, 20 fM biotin-labeled probes were incubated with the GST or GST-SPL14N protein in the binding buffer [10 mM Tris, 50 mM KCl, 1 mM EDTA, 5 mM $MgCl_2$, 1 mM DTT, 50 ng/μl Poly (dI.dC), 2.5% Glycerol and 0.05% NP-40] for 30 min at room temperature. For competition reaction, 2 pM (100×) and 4 pM(200×) un-labeled probes were mixed with the labeled probes. The DNA-protein complex was separated by 6% native polyacrylamide gel electrophoresis at 4℃. After separation, the signal of biotin was developed using the Chemiluminescent Nuleic Acid Detection Module (Thermo, USA) according to the manufacturer's protocol.

Y1H Assay

For Y1H assay, the plasmid *GAD-SPL14* was co-transformed with the *LacZ* reporter constructs into the yeast strain *EGY48* mediated by PEG. The transformants were

grown and selected on the SD/-Trp/-Ura medium (Clontech, USA), positive clones were transferred to the medium containing raffinose, galactose, IPTG and 5-Bromo-4-chloro-3-indolyl-β-D-galactopyranoside (Sigma, USA) for developing the blue color.

Y2H Assay

For Y2H assay, the *GAD* and *GBD* fusion constructs were co-transformed into the yeast strain *AH109* mediated by PEG. The transformants were grown and selected on the SD/-Trp/-Leu medium (Clontech, USA), positive clones were transferred to the SD/-Trp/-Leu/-His/-Ade medium containing 60 mM 3-Amino-1,2,4-triazole for detecting interaction.

ChIP-PCR assay

For ChIP assay, a weak line *SPL14GFP*-2, in which *SPL14* was up regulated only about 4 folds compared with WT, was chosen to avoid possible artifact caused by overexpression. The ChIP assay was performed according to the previously description (8). ~1.5-2 g young panicles (<10 mm in length) were harvested and crosslinked with 1% formaldehyde. Chromatin complexes were isolated and sonicated. The immunoprecipitation was performed using anti-GFP (Abcam, Hongkong, China) and IgG protein respectively. The precipitated and input DNA was recovered and analyzed using quantitative PCR. The values were normalized to the input firstly, and divided by the *Ubi:GFP* value to get the enrichment fold. The DNA fragment without *GTAC* motif of *actin* gene was used as the negatively control.

LUC Activity Assay

Protoplast isolation and transient expression were conducted as described (2). For protein-protein interaction, plasmids of N- and C-terminal LUC fusion genes were co-transformed with *35S:GUS* by the ratio of 10:10:1, with the latter as the internal control. For detecting the effect of *miR529* on SPL genes and the transcriptional repressor activities of *SNB* and *OsIDS1*, the plasmids containing reporters and effectors were co-transformed with *35S:GUS* by the ratio of 5:4:1, with GUS activity as the internal control. The GUS fluorescence was measured using UV fluorescence optical kit (Promega, USA), LUC activity was detected with LUC assay substrate

(Promega, USA) after 20 h incubation. Relative activity of the LUC reporter was expressed as the ratio of LUC to GUS.

BiFC

For BiFC assay, the plasmids of *ASP1-nYFP*， *SNB-cYFP* and controls were co-transformed with the *P19* silencing suppressor into *Nicotiana benthamiana* leaves by *Agrobacterium* (*GV3101* strain) infiltration (9). The infiltrated tobacco leaves were observed for imaging using confocal microscope 4 d after infiltration.

Histological Sectioning

For paraffin sectioning, the shoot apexes were collected from WT, *miR156OE*, *MIM156*, *SPL14Ri* and *SPL14OE* plants at 7 and 15 d after germination respectively. The samples were fixed in FAA solution (formaldehyde:glacial acetic acid: ethanol=1:1:18, v/v/v)for 24 h at 4℃, then dehydrated and cleared in a graded ethanol and xylene series. The samples were sectioned at 8-10 μm thickness by microtome, and the sections were stained with 0.5% toluidine blue O for 5 min at room temperature and observed with a light microscope.

In situ Hybridization

Sample fixation and sectioning were performed as described above. Hybridization and immunological detection were performed as described previously (10). The probes for *OSH1* and *FZP* were amplified by PCR using the gene-specific primers. T7 and SP6 promoters were fused to the forward and reverse primers respectively, and the PCR products were directly used to transcribe the antisense and sense probes in vitro by SP6 and T7 RNA polymerase respectively, using the digoxigenin-labeled nucleotide mixture (Sigma, USA)

Scanning Electron Microscopic Observation

Young panicles were collected from WT, *miR156OE*, *MIM172* plants by removing the surrounding leaves under stereoscope. After sampling, the tissues were fixed in 2.5% glutaraldehyde overnight at 4℃. After rinsing, the tissues were post-fixed in 1% osmium tetroxide for 2 h at 4℃, and then were critical-point dried, coated with platinum powder, and observed under the scanning electron microscope.

Microarray Analysis

RNA samples were collected from the young panicles (<1 mm) of *miR156OE* and WT plants. RNA extraction, microarray hybridization and measurement of expression levels were performed by the CapitalBio Corporation (China) using the Affymetrix system. The program R was used for the statistical analysis.

Accession Numbers

Sequence data from this article can be found in the Rice Genome Annotation Project website (MSU) or miRBase/TAIR data libraries under the following accession numbers:

SPL7 (LOC_Os04g46580), *SPL14* (LOC_Os08g39890), *SPL17* (LOC_Os09g31438), *SNB* (LOC_Os07g13170), *OsIDS1* (LOC_Os03g60430), *OsTOE1* (LOC_Os05g03040), *ASP1* (LOC_Os08g06480), *TRP1* (LOC_Os03g14980), *RCN1* (LOC_Os11g05470), *LAX1* (LOC_Os01g61480), *RFL* (LOC_Os04g51000), *PAP2* (LOC_Os03g54170), *miR156d* (MI0000656), *miR529a* (MI0003202), *miR529b* (MI0005804), *miR172b* (MI0001140), *miR172d* (MI0001154), *AtmiR172a* (At2g28056), *AtIPS1* (At3g09922), *Ubi* (LOC_Os03g13170), *Tb1* (LOC_Os03g49880), *LOG* (LOC_Os01g40630), *Ghd7* (LOC_Os07g15770), *FZP* (LOC_Os07g47330), *MADS14* (LOC_Os03g54160).

References

1. Yuan B, Shen X, Li X, Xu C, Wang S (2007) Mitogen-activated protein kinase OsMPK6 negatively regulates rice disease resistance to bacterial pathogens. *Planta* 226(4):953-960.

2. Tang W, et al. (2012) Transposase-derived proteins FHY3/FAR1 interact with PHYTOCHROME-INTERACTING FACTOR1 to regulate chlorophyll biosynthesis by modulating HEMB1 during deetiolation in *Arabidopsis*. *Plant Cell* 24(5):1984-2000.

3. Chen H, et al. (2008) Firefly luciferase complementation imaging assay for protein-protein interactions in plants. *Plant Physiol* 146(2):368-376.

4. Lin YJ, Zhang Q (2005) Optimising the tissue culture conditions for high efficiency

transformation of *indica* rice. *Plant Cell Rep* 23(8):540-547.

5. Weng X, et al. (2014) *Grain number*, *plant height*, *and heading date7* is a central regulator of growth, development, and stress response. *Plant Physiol* 164(2):735-747.

6. Livak KJ, Schmittgen TD (2001) Analysis of relative gene expression data using real-time quantitative PCR and the 2(-Delta Delta C(T)) Method. *Methods* 25(4):402-408.

7. Shen J, Xie K, Xiong L (2010) Global expression profiling of rice microRNAs by one-tube stem-loop reverse transcription quantitative PCR revealed important roles of microRNAs in abiotic stress responses. *Mol Genet Genomics* 284(6):477-488.

8. Zhao Y, Hu Y, Dai M, Huang L, Zhou DX (2009) The WUSCHEL-related homeobox gene *WOX11* is required to activate shoot-borne crown root development in rice. *Plant Cell* 21(3):736-748.

9. Voinnet O, Rivas S, Mestre P, Baulcombe D (2003) An enhanced transient expression system in plants based on suppression of gene silencing by the p19 protein of tomato bushy stunt virus. *Plant J* 33(5):949-956.

10. Xue W, et al. (2008) Natural variation in *Ghd7* is an important regulator of heading date and yield potential in rice. *Nat Genet* 40(6):761-767.

11. Kyozuka J, Tokunaga H, Yoshida A (2014) Control of grass inflorescence form by the fine-tuning of meristem phase change. *Curr Opin Plant Biol* 17:110-115.

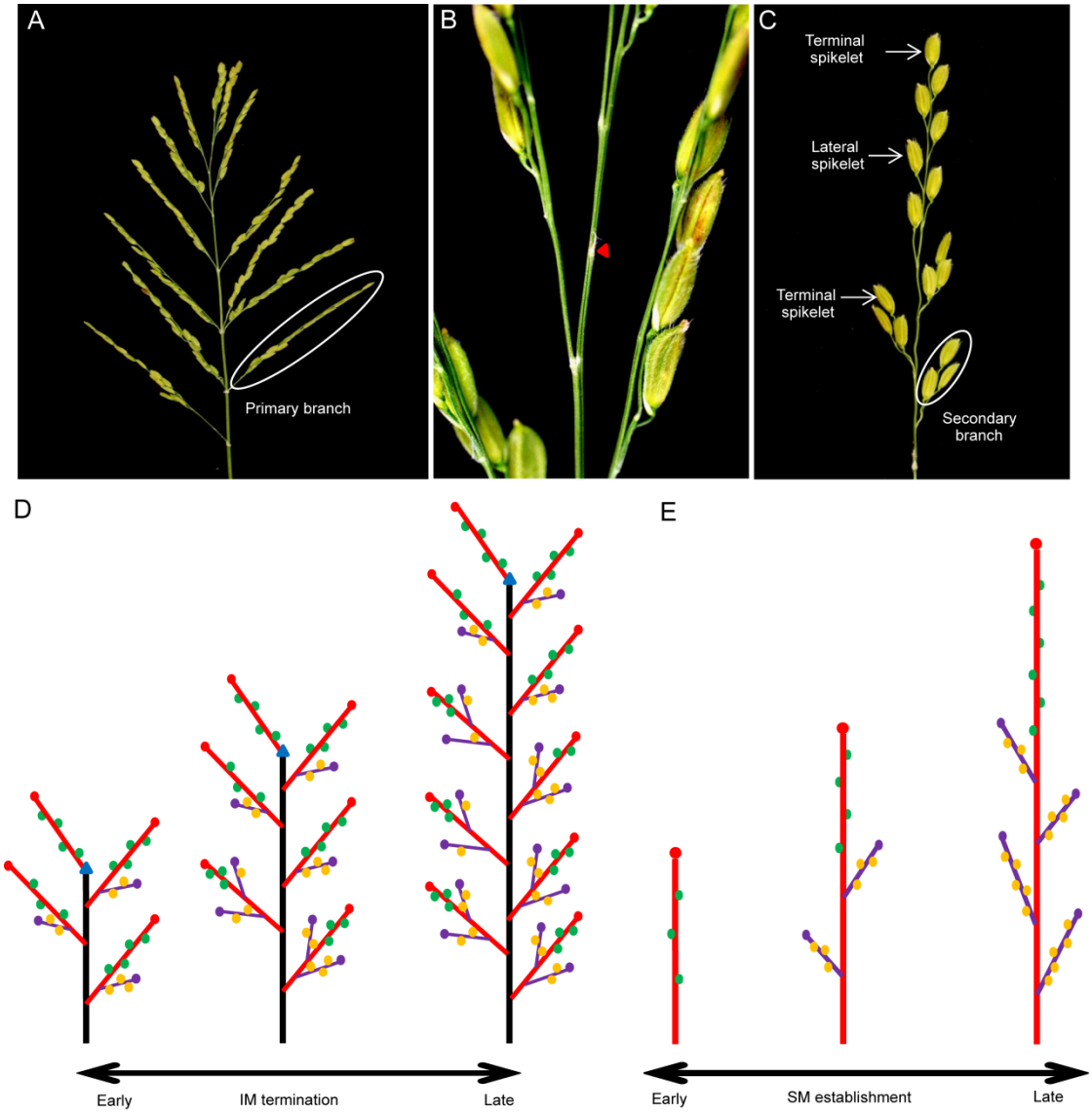

Fig. S1. Panicle morphology and development of rice.

After reproductive transition, the shoot apical meristem is converted to inflorescence meristem (IM). An IM produces several primary branches (PB) directly attached to the rachis before its termination (*A*). IM absorption leaves a vestige at the base of the uppermost PB (*B*, indicated with the red triangle). A PB produces several lateral meristems before converting to the termianl spikelet (*C*). Early arising lateral mesitems from PB develop as secondary branches (SB), whereas later arising lateral meristems of PB become specified directly as lateral spikelets. A SB also produces lateral spikelets before coverting to the termianl spikelet. The timing of IM absorption determines the number of PBs. More PBs are generated if the IM termination is delayed, and the reverse is the case for precocious IM termination (*D*). The timing of

transtion from branch meristem to spikelet meristem (SM) determines the lateral organs of PB. Precocious specification of SM results in less SBs on the PB, whereas delayed transition leads to more SBs, even higher order branches (*E*). (*D* and *E*), the blue triangles indicate the vestige points of IM; the black, red and purple lines indicate the main rachis, PB and SB respectively; red and purple dots indicate the terminal spikelets converted from PB and SB respectively; green and orange dots indicate the lateral spikelets transited from PB and SB respectively. (*D* and *E*) are adapted from Kyozuka et al (11).

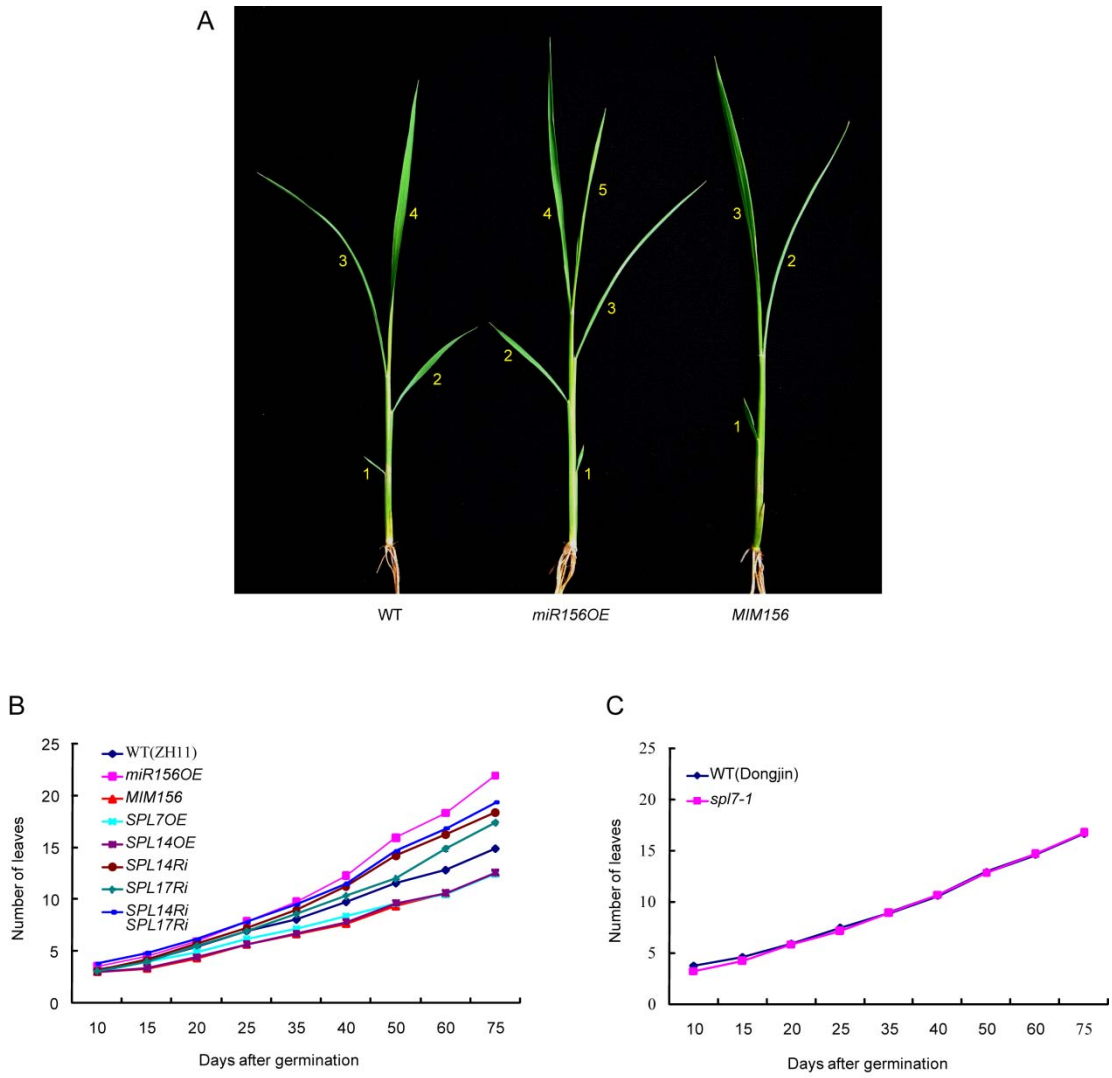

Fig. S2. The effects of *miR156* and SPL genes on plastochron length.

(*A*) The plants of WT, *miR156OE* and *MIM156* plants at 15 d after germination. The numbers indicated the leaves according to their developmental orders. (*B* and *C*) Emergence of visible leaves in the plants of various transgenes in Zhonghua 11 (*B*) and Dongjin (*C*) genetic backgrounds. Values are means ± SEM (n = 15).

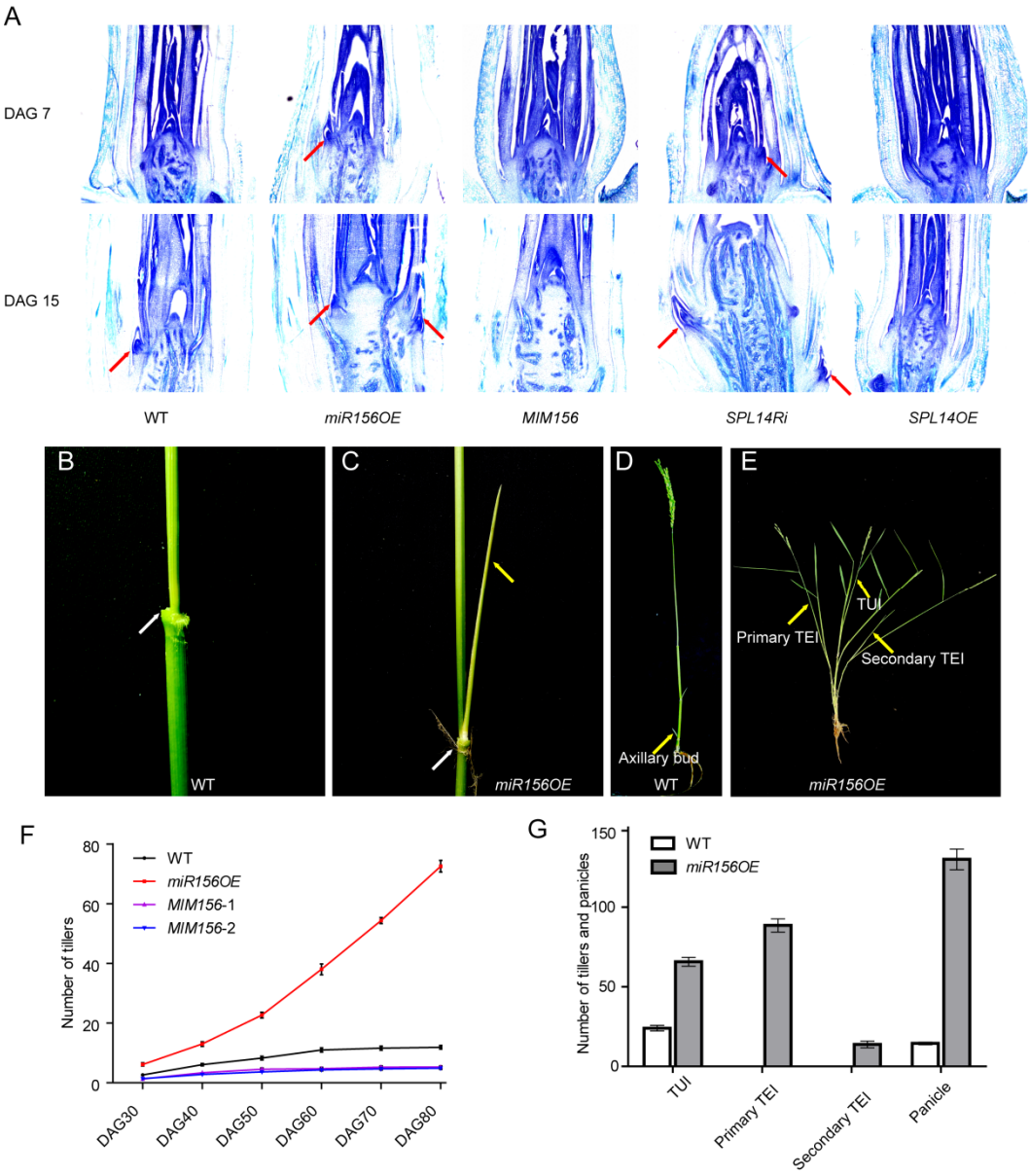

Fig. S3. Regulation of initiation and outgrowth of vegetative branching by *miR156* and SPL genes.

(*A*) Longitudinal sections of the shoot apex in WT, *miR156OE*, *MIM156*, *SPL14Ri* and *SPL14OE* plants. The red arrows indicate the tiller buds. DAG, days after germination. (*B* and *C*) Comparison of tiller buds in *miR156OE* and WT plants. No axillary bud is generated from the node (indicated by a white arrow) of the flag leaf in WT (*B*), but a visible tiller bud (indicated by a yellow arrow) at that node in *miR156OE* plants (*C*). (*D* and *E*) Comparison of axillary buds in *miR156OE* and WT plants. Axillary buds formed from the elongated upper internodes are dormant in WT (*D*), whereas *miR156OE* plants produces extra tillers from these elongated upper

internodes (*E*). TUI, tillers formed by un-elongated internodes; TEI, tillers formed from the elongated internodes. (*F*) Number of tillers per plant at different time points in WT, *miR156OE* and *MIM156*. DAG, days after germination. Values are means ± SEM (n = 15). (G) Comparison of tiller numbers between WT and *miR156OE* plants at maturation stage. Values are means ± SEM (n = 10).

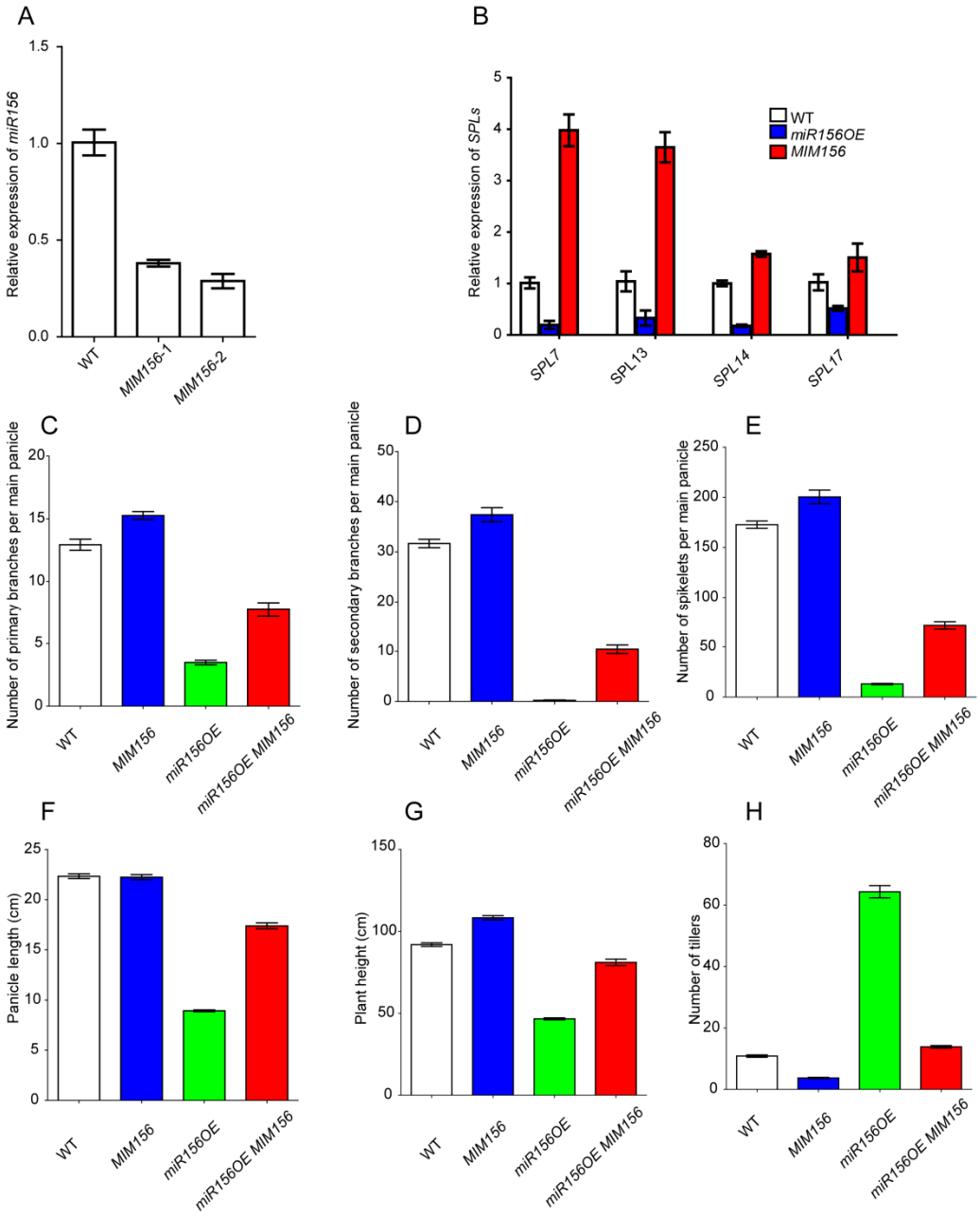

Fig. S4. The effects of interfering the activity of *miR156* by target mimicry.

(*A*) Relative abundance of *miR156* in the plumule of *MIM156* plants compared with WT. Values are means ± SEM (n = 3). (*B*) Relative abundance of *SPL7*, *SPL13*, *SPL14* and *SPL17* in the axillary bud of WT, *miR156OE* and *MIM156* plants. Values are means ± SEM (n = 3). (*C-H*) Measurements of plant and panicle morphology traits in the WT, *MIM156*, *miR156OE* and the hybrid between *miR156OE* and *MIM156* plants: numbers of primary branches (*C*), secondary branches (*D*), spikelets (*E*), panicle length (*F*), plant height (*G*) and tiller number (*H*).Values are means ± SEM (n = 15).

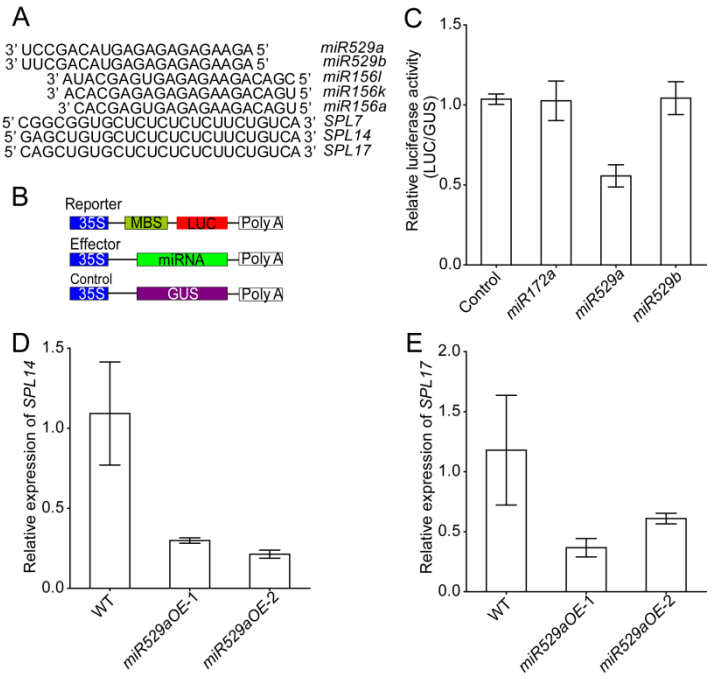

Fig. S5. SPL genes were also regulated by *miR529a*.

(*A*) Sequence alignment of *miR156*, *miR529* and their recognizing sites in SPL genes. (*B*) Schematic diagram of reporter and effector constructs used in the LUC assay for investigating the effects of *miR529* on the SPL genes. MBS, microRNA binding site. (*C*) Relative LUC activites in *Arabidopsis* protoplast transformed with different constructs. Datas are normalized to the internal control *35S:GUS* co-transformed in the assay. Values are means ± SEM (n = 3). (*D* and *E*) Relative expression of *SPL14* (*D*) and *SPL17* (*E*) in WT and *miR529aOE* plants. Values are means ± SEM (n = 3).

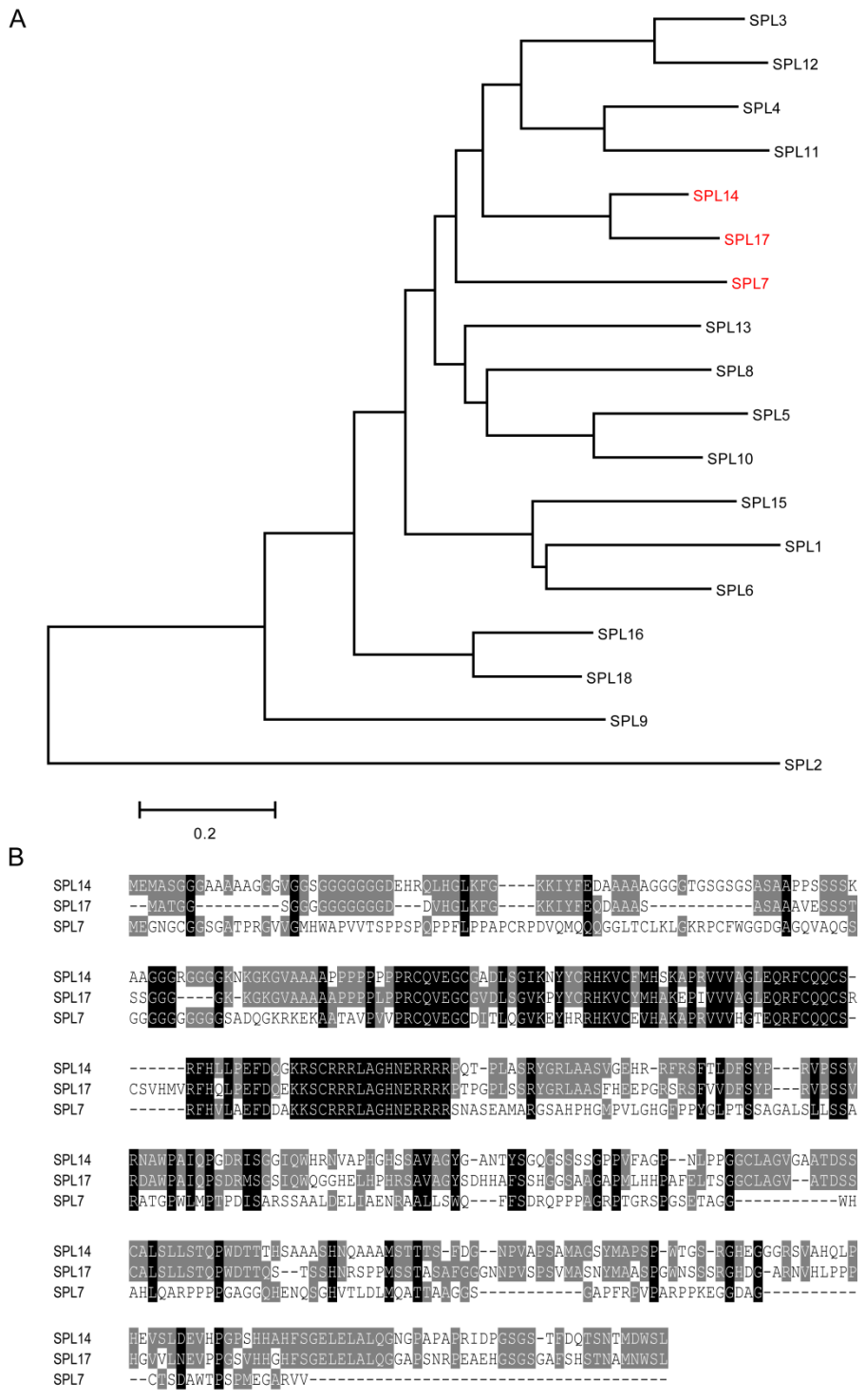

Fig. S6. Phylogenetic tree and multiple sequence alignment of SPL proteins.

(*A*) Phylogenetic tree of all the 18 rice SPL protein sequences using the neighbor-joining method. (*B*) Multiple sequence alignment of SPL7, SPL14 and SPL17 proteins.

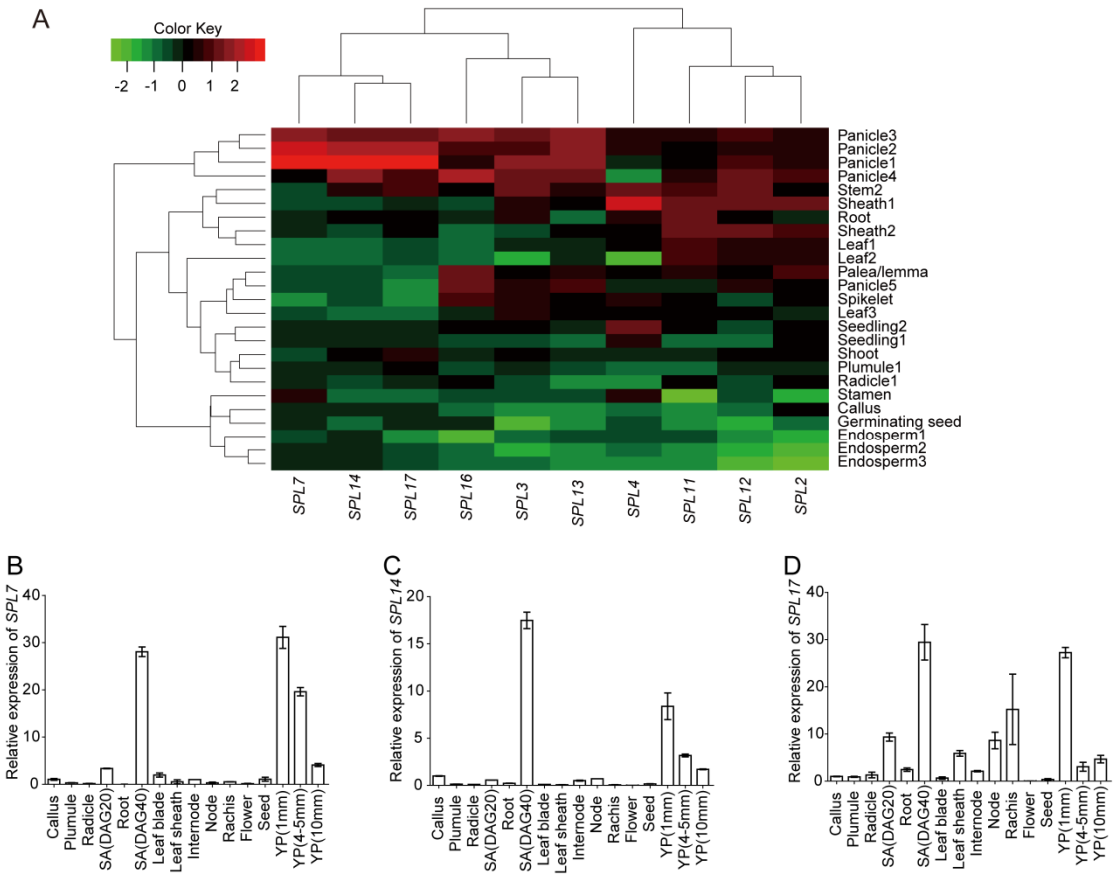

Fig. S7. Expression features of SPL genes.

(*A*) Hierarchical clustering of the expression patterns of 10 rice SPL genes targeted by *miR156*. The data are the microarray values of 25 tissues of the rice variety Minghui 63 extracted from the database CREP (http://crep.ncpgr.cn). (*B-D*) The relative expression levels of *SPL7* (*B*), *SPL14*(*C*) and *SPL17* (*D*) in 16 tissues collected from Zhonghua 11. Values are means ± SEM (n = 3); SA, shoot apex; YP, young panile; DAG, days after germination. Callus was collected 20 d after subculture; plumule and radicle were collected 48 h after germination; root, leaf blade, leaf sheath, internode, node, rachis and flower were collected at heading stage; seeds were collected 7 d after flowering.

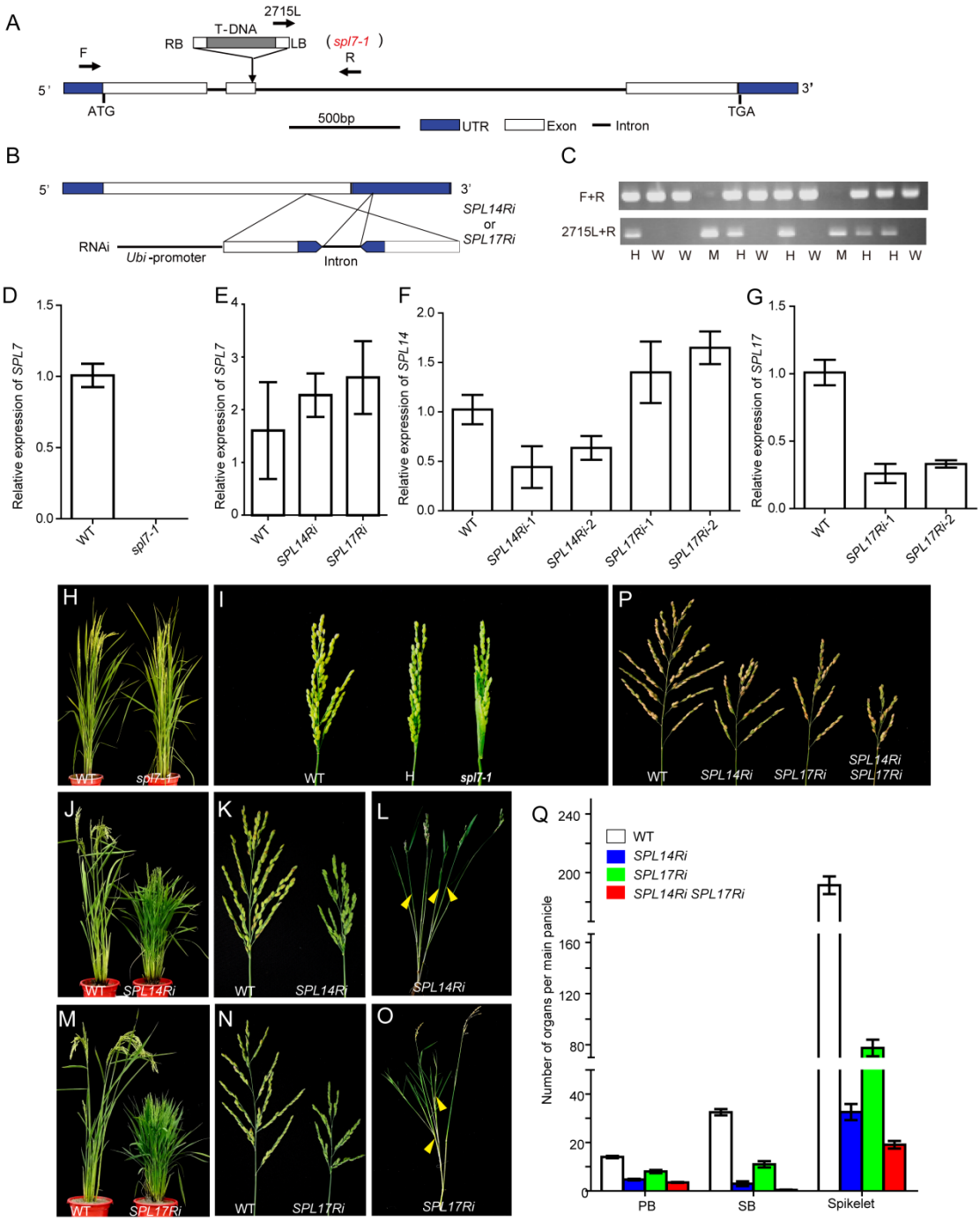

Fig. S8. Effects of *SPL7*, *SPL14* and *SPL17* on tillering and panicle branching investigated by down-regulating the genes.

(*A*) Schematic diagram of gene structure of *SPL7* and T-DNA insertion site in *spl7-1*. LB and RB indicate the left and right borders of T-DNA. F, R and 2715L indicate the primers used for detection of T-DNA insertion. (*B*) Schematic diagram of the RNAi constructs of *SPL14* and *SPL17*. The white box indicates the exon, whereas the blue box indicates the UTR region. (*C*) PCR results of genotyping the mutant *spl7-1*. W, M

and H indicate the WT, homozygote of T-DNA insertion and the hemizygote respectively. (*D*-*G*) Relative expression of *SPL7* (*D* and *E*), *SPL14* (*F*) and *SPL17* (*G*) in the flag leaf of their corresponding mutant or RNAi lines compared with WT. Values are means ± SEM (n = 3). (*H* and *I*) The plants (*H*) and panicles (*I*) of WT and *spl7-1* mutant. H indicates the hemizygote of T-DNA insertion. (*J*-*O*) The plants (*J*, *M*), panicles (*K*, *N*) and higher order tillers (*L*, *O*) of *SPL14Ri* (*J* and *L*) and *SPL17Ri* (*M* and *O*) plants. Arrowhead indicates the tillers formed from eloanged upper internodes. (*P* and *Q*) The panicles (*P*) and statistical comparison (*Q*) of WT, *SPL14Ri*, *SPL17Ri* and the hybrid between *SPL14Ri* and *SPL17Ri* plants. Values are means ± SEM (n = 10). PB, primary branch; SB, secondary branch.

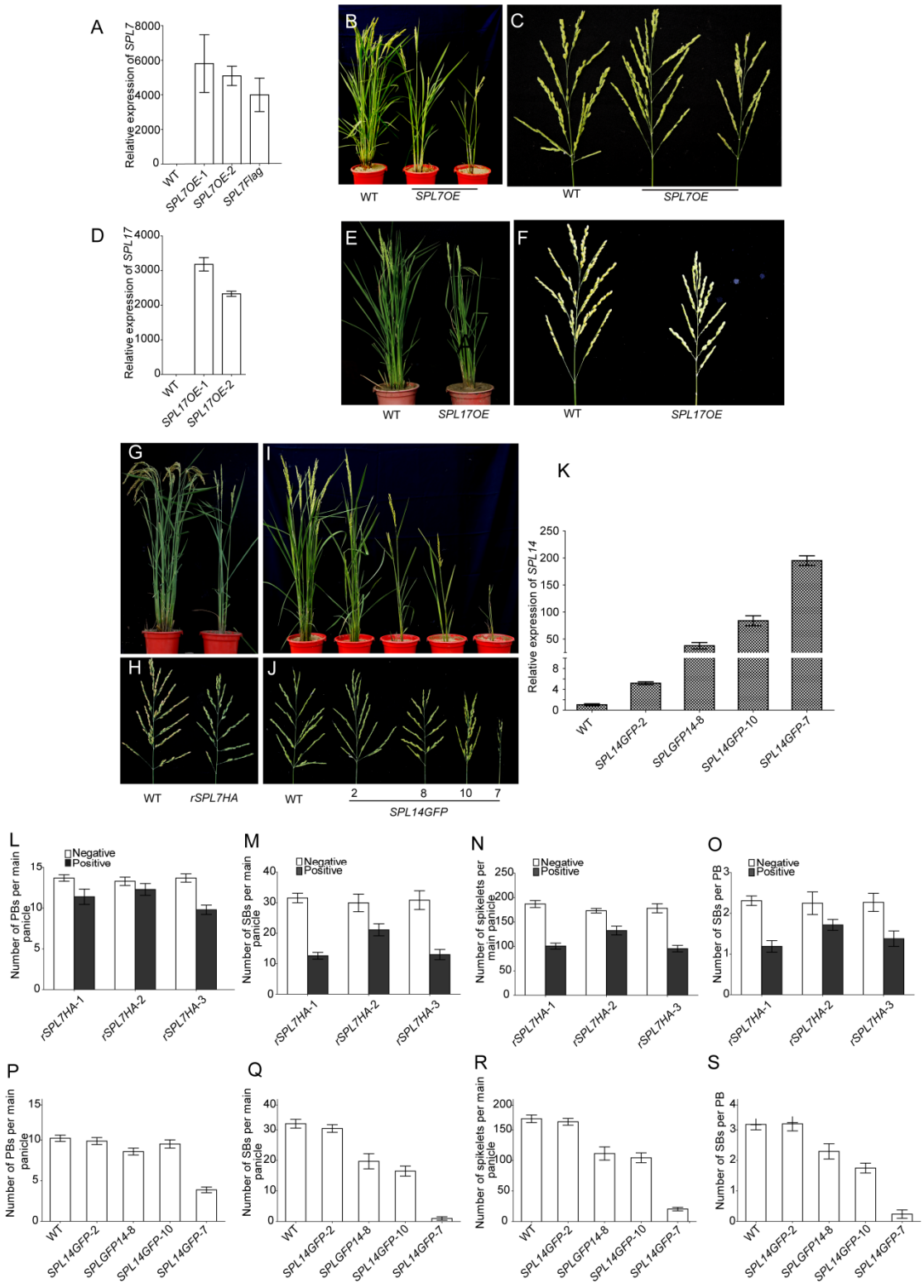

Fig. S9. Phenotypes of *SPL7OE*, *SPL17OE*, *rSPL7HA* and *SPL14GFP* transgenic plants.

(*A*) Relative expression levels of *SPL7* in flag leaf of its overexpressing plants. Values are means ± SEM (n = 3). (*B* and *C*) The plants (*B*) and panicles (*C*) of *SPL7OE*

compared with WT. (*D*) Relative expression levels of *SPL17* in flag leaf of its overexpressing plants. Values are means ± SEM (n = 3). (*E* and *F*) The plants (*E*) and panicles (*F*) of *SPL17OE* compared with WT. (*G-J*) Plants (*G*, *I*) and panilces (*H*, *J*) of *rSPL7HA* (*G* and *H*) and *SPL14GFP* (*I* and *J*) transformants. (*K*) Relative expression level of *SPL14* in flag leaf of *SPL14GFP* trangenic plants. Values are means ± SEM (n = 3). (*L-S*) Measurements of panicles in *rSPL7HA* (*L-O*) and *SPL14GFP* (*P-S*). PB, primary branch; SB, secondary branch. Values are means ± SEM (n = 10 for *rSPL7HA*; n = 6-14 for *SPL14GFP*).

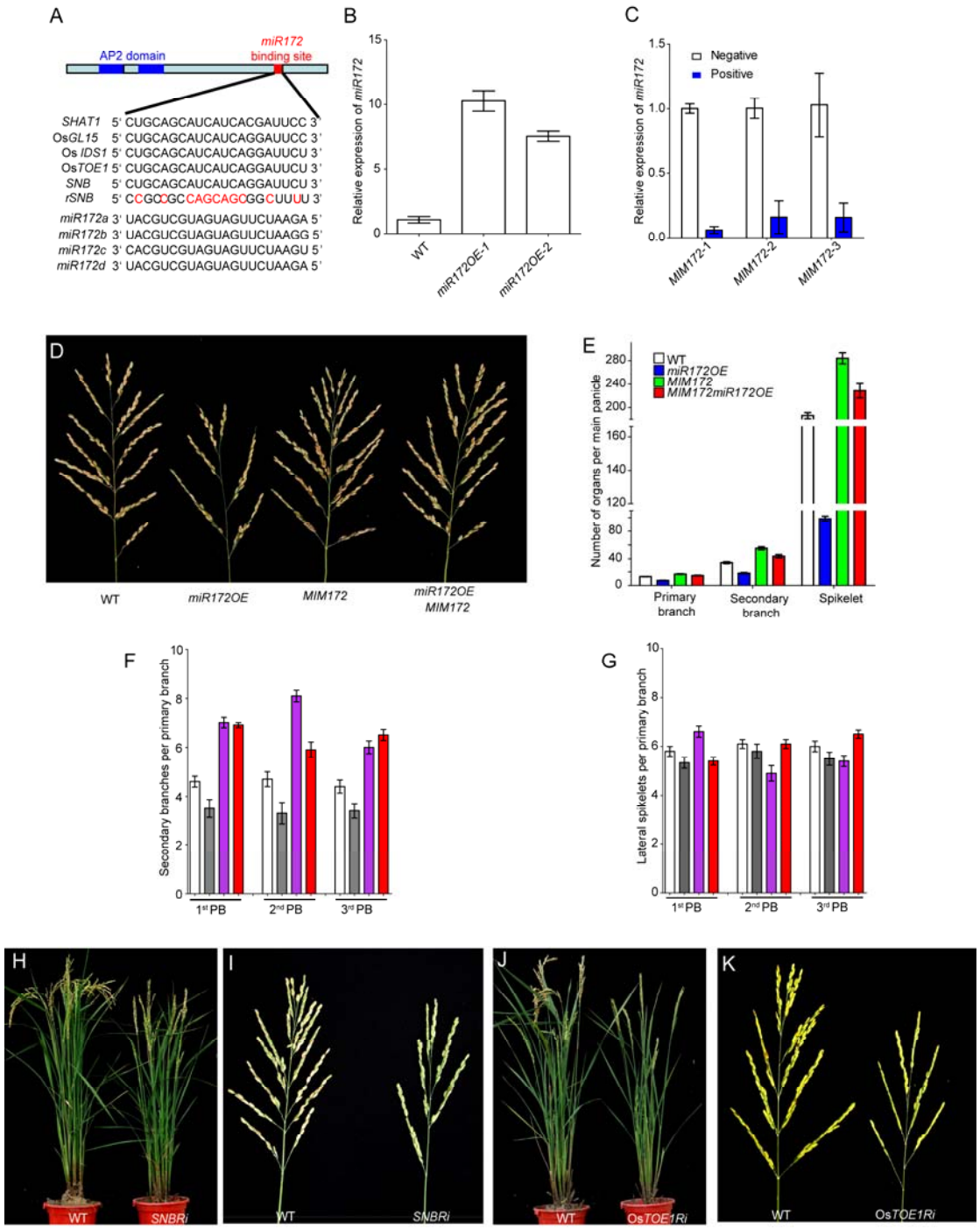

Fig. S10. The roles of *miR172* and its target genes on the rice tillering and panicle branching.

(*A*) Sequence of *miR172* and its recognizing sites in the target genes. The red letters in the *rSNB* indicate the changed nucleotides but not the amino acids for preparing the *miR172*-resistant *SNB*. (*B* and *C*) Relative expression of mature *miR172* in *miR172OE* (*B*) and *MIM172* (*C*) plants. Vaules are means ± SEM (n = 3). (*D* and *E*) Morphology (*D*) and measurements (*E*) of the panicles of WT, *miR172OE*, *MIM172* and the hybrid

between *miR172OE* and *MIM172*. Values are means ± SEM (n = 10). (*F* and *G*) Numbers of secondary branches (*F*) and lateral spikelets (*G*) generated by each primary branch in WT (white), *miR172OE* (gray), *MIM172* (purple) and *rSNBOE* (red) plants. Three groups of histograms indicate the data from the first, second and third primary branches of the panicle respectively. Values are means ± SEM (n = 10). (*H-K*) Plants (*H*, *J*) and panicles (*I*, *K*) of the RNAi lines of *SNB* (*H* and *I*) and Os*TOE1* (*J* and *K*) compared with WT.

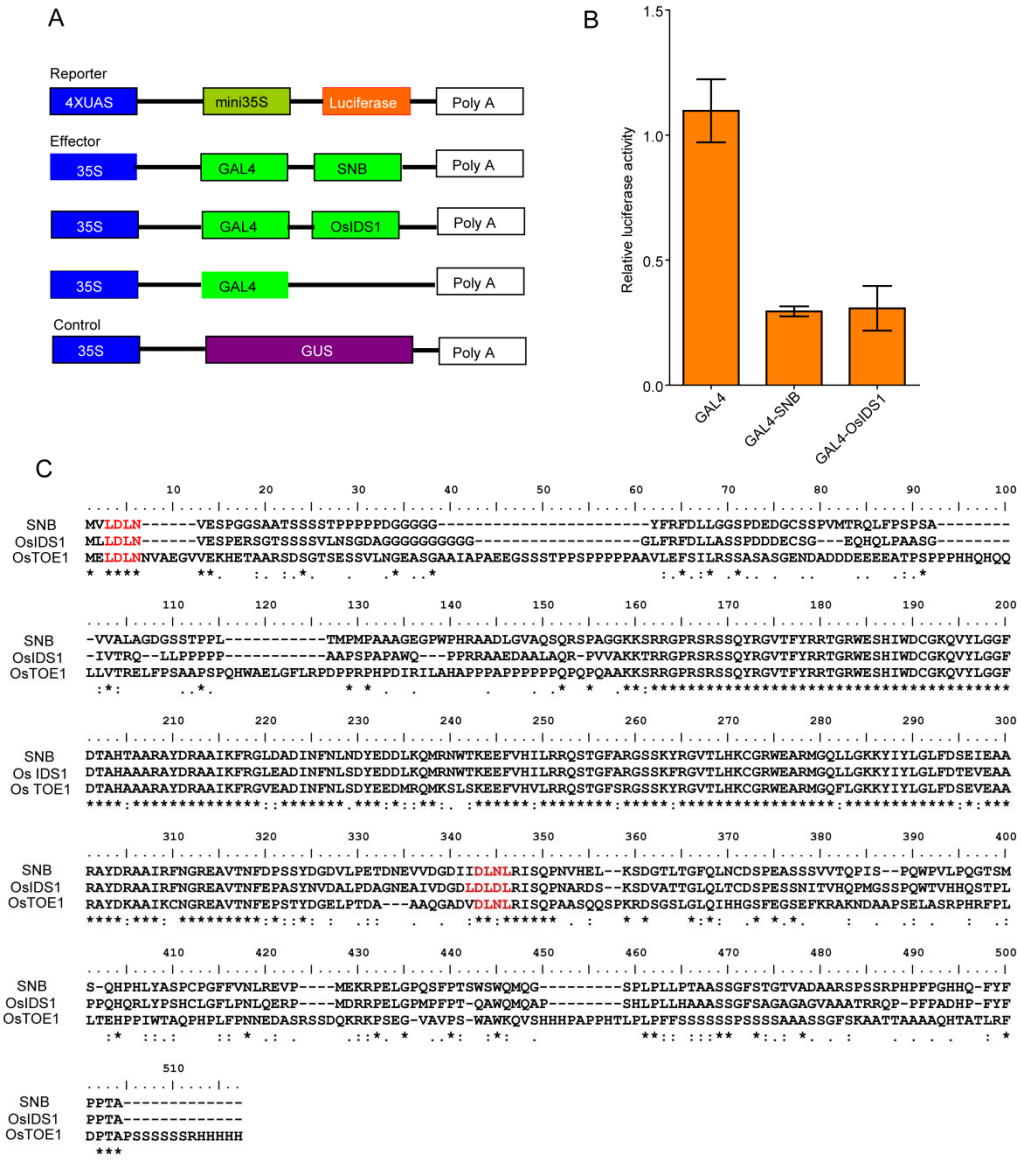

Fig. S11. Transcriptional activities and protein sequences of SNB, OsIDS1 and OsTOE1.

(*A*) Schematic diagram of reporter and effector constructs used in the LUC assay for transcriptional activity. (*B*) Relative LUC activites in *Arabidopsis* protoplast transformed with different constructs. Data are normalized to the internal control *35S:GUS*, which was co-transformed in the assay. Values are means ± SEM (n = 3). (*C*) Multiple sequence alignment of SNB, OsIDS1 and OsTOE1 proteins. Red letters indicate the two putative EAR motifs.

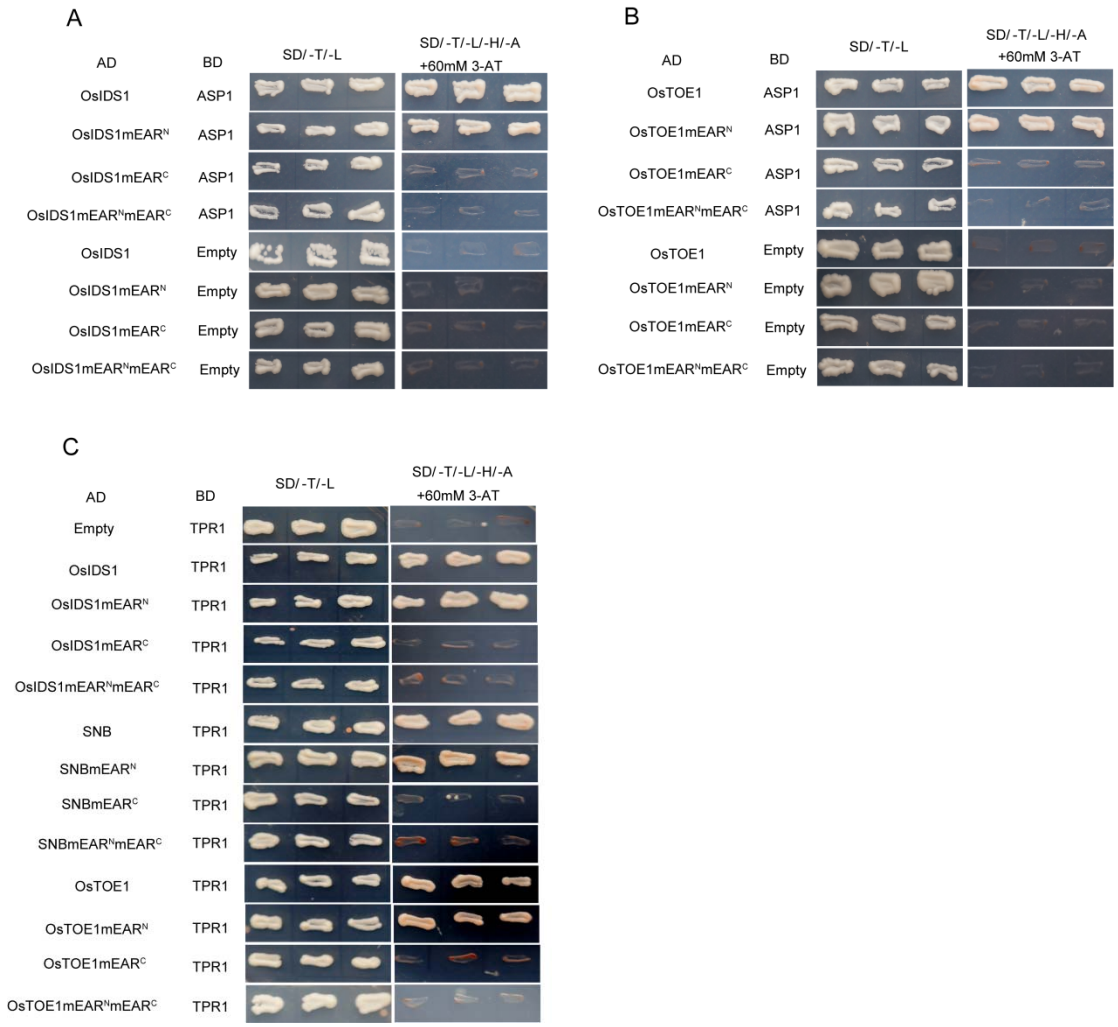

Fig. S12. Protein interaction assays of SNB, OsIDS1, OsTOE1 and ASP1 or TPR1.

(*A*) Y2H assay for interaction between OsIDS1 (native or with mutated EAR motif) and ASP1 in yeast. The co-transformation clones were screened on the plate without Trp (T) and Leu (L) fisrstly, then the protein interactions were examined on the plate withou T, L, His (H), Adenine (A) but with 60 mM 3-AT. AD, GAL4 activation domain; BD, GAL4 DNA binding domain. (*B*) Y2H assay for interaction between OsTOE1 (native or with mutated EAR motif) and ASP1 in yeast. All selection conditions are as in (A). (*C*) Y2H assay for interactions between OsTOE1, SNB, OsTOE1 (native or with mutated EAR motif) and TRP1 in yeast. All selection conditions are as in (*A*).

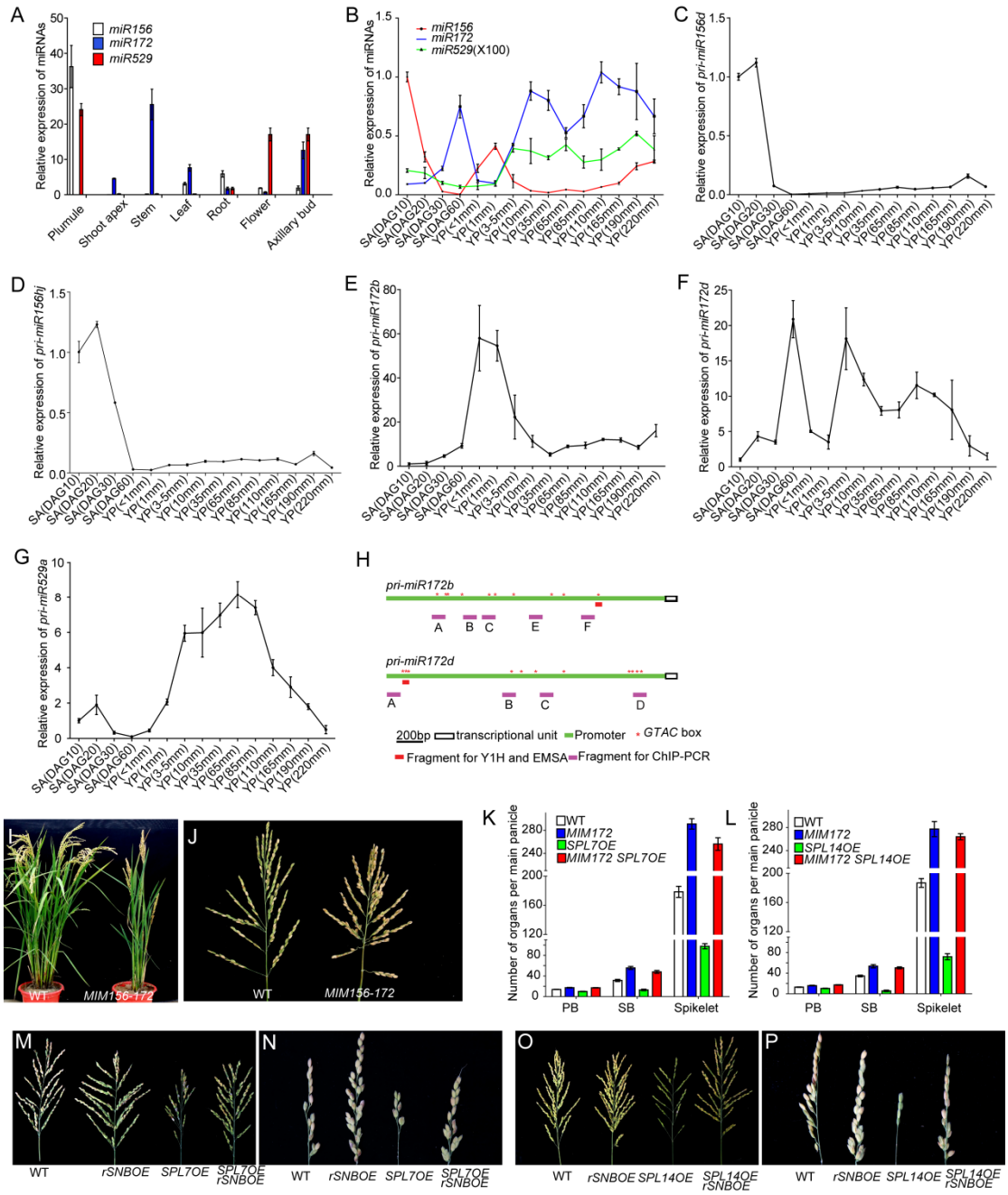

Fig. S13. *SPL*s positively regulated spikelet transition by *miR172-AP2* pathway.

(*A*) Relative expression levels of *miR156*, *miR172* and *miR529* in various tissues. Plumules were collected 48 h after germination; shoot apex and roots were collected 40 d after germination; leaf, stem and flower were collected at heading stage; axillary buds were collected in 1-5 mm length. Vaules are means ± SEM (n = 3). (*B*) Relative expression levels of mature *miR156*, *miR172*, *miR529* in shoot apex (SA) and developing young panicles (YP) at various time points. Vaules are means ± SEM (n = 3). DAG, days after germination. (*C*-*G*) Relative expression levels of the precursors

of *miR156* (*C* and *D*), *miR172* (*E* and *F*), *miR529* (*G*) in shoot apex (SA) and developing young panicles (YP) at various time points. Vaules are means ± SEM (n = 3). DAG, days after germination. (*H*) Schematic diagram of the promoters and the fragments of *pri-miR172b* and -*miR172d* for Y1H, EMSA and ChIP assay. (*I* and *J*) Plants (*I*) and panicles (*J*) of WT and *MIM156-172* transformant. (*K* and *L*) The measurements of the panicles of WT, *SPL7OE*, *SPL14OE*, *MIM172* and the corresponding hybrids. Vaules are means ± SEM (n = 10). PB, primary branch; SB, secondary branch. (*M* and *N*) Panicles (*M*) and primary branches (*N*) of WT, *rSNBOE*, *SPL7OE* and the hybrid between *rSNBOE* and *SPL7OE*. (*O* and *P*) Panicles (*O*) and primary branches (*P*) of WT, *rSNBOE*, *SPL14OE* and the hybrid between *rSNBOE* and *SPL14OE*.

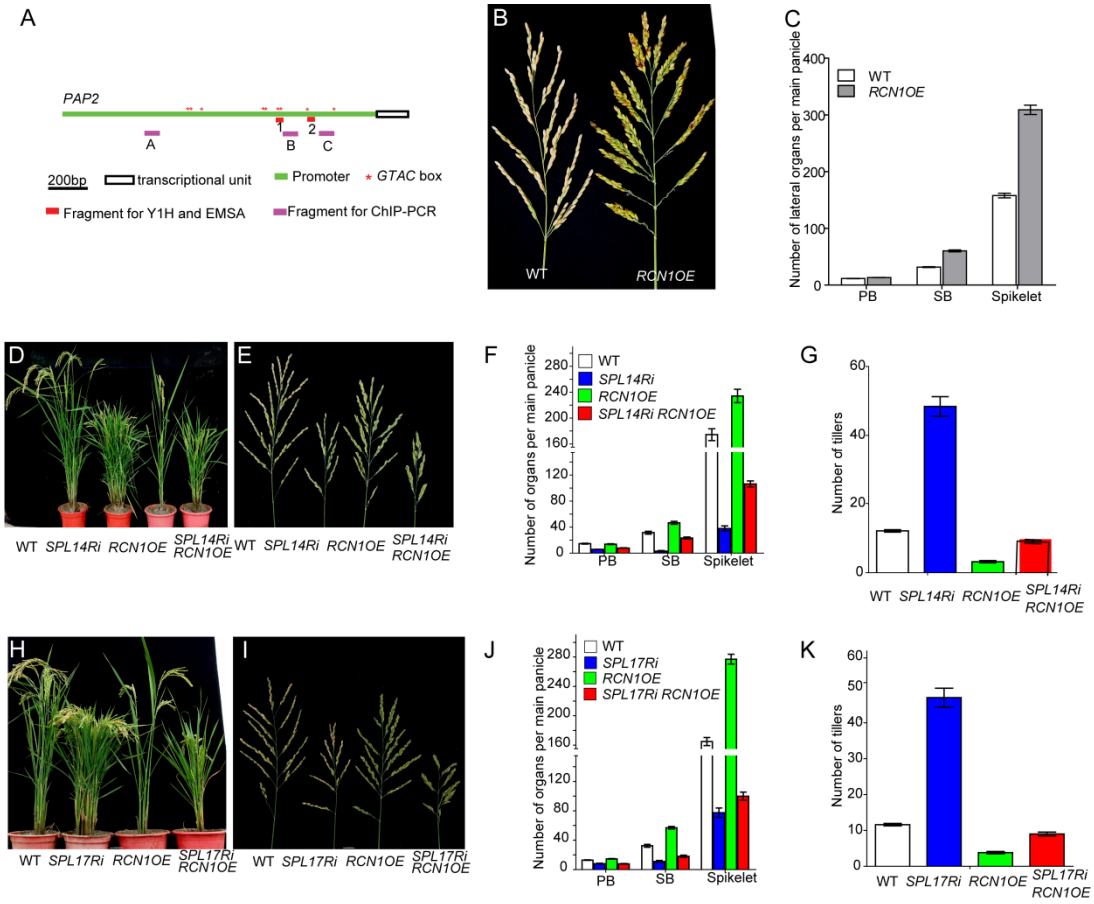

Fig. S14. *SPL*s also regulated spikelet transition through *PAP2*/*MADS34*-*RCN* pathway.

(*A*) Schematic diagram of the promoter and the fragments of *PAP2* for Y1H, EMSA and ChIP assays. (*B* and *C*) Panicles (*B*) and measurements (*C*) of *RCN1OE* compared with WT. Values are means ± SEM (n = 10). PB, primary branch; SB, secondary branch. (*D*-*G*) Morphology of plants (*D*) and panicles (*E*), and the measurements of panicles (*F*) and tillers (*G*) of WT, *SPL14Ri*, *RCN1OE* and the corresponding hybrids. Values are means ± SEM (n = 10). PB, primary branch; SB, secondary branch. (*H*-*K*) Morphology of plants (*H*) and panicles (*I*), and the measurements of panicles (*J*) and tillers (*K*) of WT, *SPL17Ri*, *RCN1OE* and the corresponding hybrids. Values are means ± SEM (n = 10). PB, primary branch; SB, secondary branch.

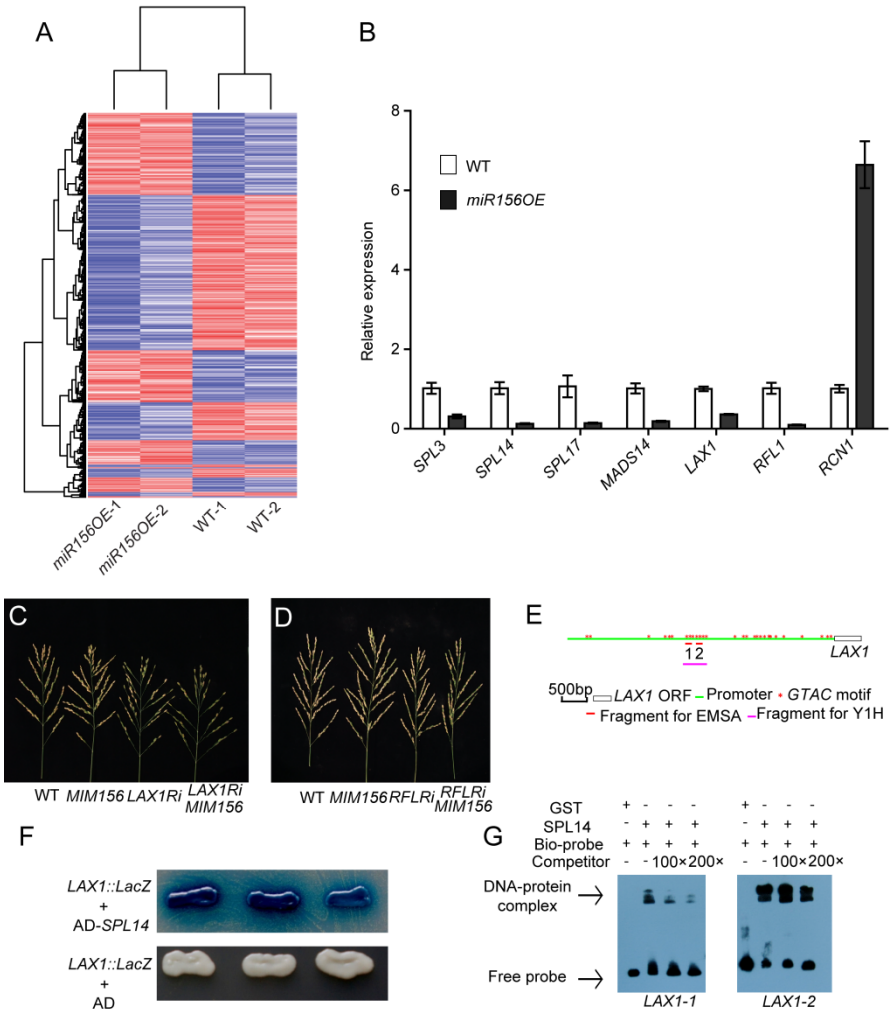

Fig. S15. Integration of *LAX1* and *RFL* by *SPL*s in regulating panicle branching.

(*A*) Hierarchical clustering of differentially expressed genes detected by microarray in the young panicles (<1 mm) of *miR156OE* compared with WT plants. Blue and red indicate high and low expression values respectively. (*B*) Relative expression levels of diverse genes in the panicles (<1 mm) of *miR156OE* compared with WT. Values are means ± SEM (n = 3). (*C* and *D*) Panicles of WT, *MIM156*, *LAX1Ri*, *RFLRi* and the hybrid as indication. (*E*) Schematic diagram of the promoter and the fragments of *LAX1* for Y1H and EMSA assay. (*F*) Y1H assay of *SPL14* with the promoter of *LAX1*. The fragment is shown in (*E*). (*G*) EMSA of GST and GST-SPL14N recombinant proteins incubated with biotin-labled probes of *LAX1*. The probe fragments are shown in (*E*).

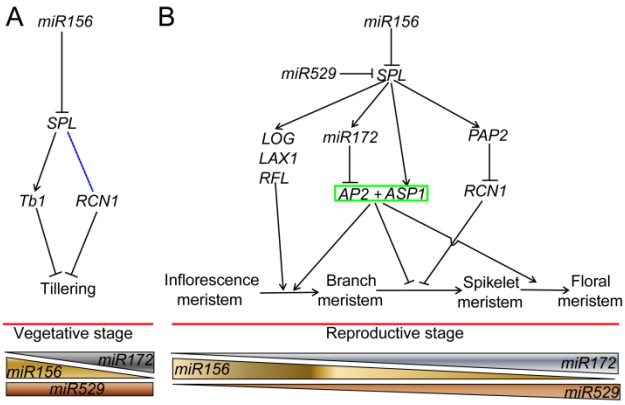

Fig. S16. A model for the coordinated regulation of vegetative and reproductive branching by *miR156*/*miR529*, *miR172* and their target genes.

Table S1. Panicle morphology of *miR156, SPL7, SPL14* and *SPL17* transgenic plants.

Genotype	No. of plants	No. of PBs	No. of SBs	No. of spikelets
WT(ZH11)	10	13.6±0.4	36.0±1.7	204.3±7.4
*miR156*OE	10	3.7±0.3^{c}	0.4±0.3^{c}	14.2±1.5^{c}
MIM156 (-)	15	12.6±0.4	21.4±0.8	139.8±4.4
MIM156-1(+)	17	16.2±0.6^{c}	25.9±1.2^{c}	171.9±5.6^{c}
MIM156-2(+)	12	16.0±0.6^{c}	22.0±2.7	155.8±6.8^{a}
WT(Dongjin)	21	10.0±0.3	15.8±1.1	107.0±4.6
spl7-1	21	10.2±0.2	16.3±0.9	120.0±4.1
*SPL14*Ri-1(-)	9	11.0±0.4	28.1±1.3	146.0±6.1
*SPL14*Ri-1(+)	16	5.3±0.2^{c}	7.8±0.6^{c}	48.2±2.2^{c}
*SPL14*Ri-2(-)	21	13.2±0.4	33.3±1.1	167.6±5.7
SPL14Ri-2(+)	24	6.1±0.3c	5.7±0.6c	43.1±2.2c
*SPL14*Ri-3(-)	12	12.4±0.2	32.0±1.2	166.7±5.4
*SPL14*Ri-3(+)	14	5.3±0.2^{c}	5.0±0.6^{c}	38.8±2.4^{c}
*SPL17*Ri-1(-)	9	14±0.4	39±1.6	205.2±7.3
*SPL17*Ri-1(+)	19	7.5±0.3^{c}	13.5±1.0^{c}	82.8±5.0^{c}
*SPL17*Ri-2(-)	10	13.4±0.6	35.9±1.5	191.7±5.5
*SPL17*Ri-2(+)	20	7.7±0.2^{c}	13.6±0.6^{c}	89.9±3.5^{c}
*SPL17*Ri-3(-)	9	14.0±0.4	40.4±1.7	202.8±6.7
*SPL17*Ri-3(+)	20	6.6±0.3^{c}	9.3±0.8^{c}	60.1±3.0^{c}
*SPL7*OE-1(-)	10	14.3±0.5	28.7±2.3	161.6±7.1
*SPL7*OE-1(+)	10	9.1±2.9^{c}	4.4±1.4^{c}	53.0±6.9^{c}
*SPL7*OE-2(-)	12	12.0±0.5	23.5±1.3	138.4±5.8
*SPL7*OE-2(+)	11	10.6±0.5^{c}	9.9±1.2^{a}	87.5±6.0^{c}
*SPL7*OE-3(-)	17	12.4±0.3	19.1±1.1	129.9±3.4
*SPL7*OE-3(+)	18	10.4±0.4^{c}	8.6±1.4^{c}	78±5.5^{c}
*SPL14*OE-1(-)	14	13.0±0.5	22.9±1.2	146.4±6.1
*SPL14*OE-1(+)	10	10.5±0.5^{b}	5.8±1.5^{c}	72.0±6.0^{c}
*SPL14*OE-2(-)	12	13.0±0.2	30.1±1.9	167.9±5.1
*SPL14*OE-2(+)	11	10.8±0.5^{b}	8.6±2.2^{c}	84.5±8.2^{c}
*SPL14*OE-3(-)	11	13.4±0.3	23.7±0.8	139.6±3.7
*SPL14*OE-3(+)	13	11.3±0.5^{b}	9.9±0.9^{c}	91.0±3.9^{c}
*SPL17*OE(-)	13	13.9±0.6	29.0±1.5	171.0±7.1
*SPL17*OE(+)	11	10.5±0.4^{c}	6.0±1.5^{c}	77.9±5.5^{c}

All data are means±SEM of main panicles. (+) and (-) indicate transgene-positive and negative respectively. *t*-test was used to compare the values between the transgene-negative and positive plants. ^{a,b,c}Statistically significant at $P<0.05$, 0.01 and 0.001 respectively. PB, primary branch; SB, secondary branch.

Table S2. Panicle morphology of *miR172*, *SNB*, and *OsTOE1* transgenic plants.

Genotype	No. of plants	No. of PBs	No. of SBs	No. of spikelets	Panicle length (cm)
*miR172*OE-1(-)	11	14.4±0.6	36.6±2.5	194.7±9.0	NA
*miR172*OE-1(+)	10	8.4±0.5^{c}	14.6±1.7^{c}	89.5±7.2^{c}	NA
*miR172*OE-2(-)	12	9.7±0.3	32.0±1.3	156.2±4.9	NA
*miR172*OE-2(+)	10	8.3±0.4^{b}	22.8±1.5^{c}	118.1±4.9^{c}	NA
*miR172*OE-3(-)	10	12.6±0.6	39.0±1.7	202.4±7.4	NA
*miR172*OE-3(+)	10	6.6±0.4^{c}	17.2±1.0^{c}	103.8±6.7^{c}	NA
MIM172-1(-)	11	13.5±0.3	34.2±1.8	185.1±6.6	23.6±0.5
MIM172-1(+)	14	16.1±0.5^{c}	54.4±2.3^{c}	278.4±9.5^{c}	18.4±0.4^{C}
MIM172-2(-)	10	12.9±0.4	34.6±1.7	186.8±6.1	23.5±0.4
MIM172-2(+)	10	17.3±0.6^{c}	55.5±2.9^{c}	289.0±10.6^{c}	19.9±0.6^{c}
*rSNB*OE-1(-)	11	11.8±0.4	30.2±1.3	170.5±6.3	21.7±0.3
*rSNB*OE-1(+)	13	11.2±0.3	41.6±1.3^{c}	221.4±6.5^{c}	19.7±0.3^{c}
*rSNB*OE-2(-)	11	12.0±0.3	26.6±1.7	157.7±6.8	22.4±0.6
*rSNB*OE-2(+)	11	13.3±0.3^{b}	47.5±2.4^{c}	253.5±9.4^{c}	19.5±0.6^{b}
*rSNB*OE-3(-)	12	11.8±0.3	31.7±1.6	176.5±8.3	20.6±0.4
*rSNB*OE-3(+)	12	12.08±0.3	46.3±1.9^{c}	246.9±8.3^{c}	19.4±0.5^{c}
*OsTOE1*OE-1(-)	6	14.7±0.7	24.3±1.6	170.8±5.4	22.2±0.6
*OsTOE1*OE-1(+)	11	15.9±0.5	33.1±2.6^{a}	193.8±6.5^{a}	20.8±0.3^{a}
*OsTOE1*OE-2(-)	7	13.0±0.4	20.0±1.7	135.1±8.7	22.3±0.2
*OsTOE1*OE-2(+)	14	13.2±0.2	27.6±2.1^{a}	165.5±5.7^{b}	21.0±0.3^{a}
*SNB*Ri-1(-)	10	13.5±0.4	23.5±2.3	158.2±8.6	NA
*SNB*Ri-1(+)	11	11.4±0.5^{c}	17.0±1.4^{a}	119.9±4.1^{c}	NA
*SNB*Ri-2(-)	11	13.0±0.4	30.2±1.0	167.9±3.1	NA
*SNB*Ri-2(+)	10	10.4±0.7^{b}	16.3±2.1^{c}	109.3±7.1^{c}	NA
*OsTOE1*Ri-1(-)	13	14.1±0.4	22.5±1.3	154.8±4.7	NA
*OsTOE1*Ri-1(+)	11	11.8±0.6^{b}	17.5±1.5^{a}	125.6±7.2^{b}	NA
*OsTOE1*Ri-2(-)	13	13.0±0.3	30.8±1.7	184.6±6.4	NA
*OsTOE1*Ri-2(+)	10	10.3±0.6^{c}	18.1±1.3^{c}	118.2±4.8^{c}	NA

All data are means±SEM of main panicles. (+) and (-) indicate transgene-positive and negative respectively. *t*-test was used to compare the values between the transgene-negative and positive plants. ^{a,b,c}Statistically significant at $P<0.05$, 0.01 and 0.001 respectively. PB, primary branch; SB, secondary branch; NA, no analysis.

Dataset S1. Global analysis of genes regulated by *miR156* overexpression in young panicles and Gene Ontology enrichment analysis.

Dataset S2. The primers used in this study.